Fungal derived 15-keto-prostaglandin E_2 activates host peroxisome proliferator-activated receptor gamma (PPAR-γ) to promote C. neoformans growth during infection.

Authors:

Robert J. Evans[1,2], Sarah Needs[3], Maceler Aldrovandi[4], Jens Tiefenbach[5], Ewa Bielska[3], Rachel E. Rubino[6], Christopher J. Nicol[6], Robin C. May[3], Henry M. Krause[5], Valerie B. O'Donnell[4], Stephen A. Renshaw[1,2], Simon A. Johnston[1,2]

[1] Bateson Centre, Firth Court, University of Sheffield, S10 2TN, UK.

[2] Department of Infection, Immunity and Cardiovascular Disease, Medical School, University of Sheffield, S10 2RX, UK.

[3] Institute of Microbiology and Infection, School of Biosciences, University of Birmingham, Birmingham, B15 2TT, UK.

[4] Systems Immunity Research Institute, and Division of Infection and Immunity, School of Medicine, Cardiff University, Cardiff CF14 4XN, UK

[5] Banting and Best Department of Medical Research, The Terrence Donnelly Centre for Cellular and Biomolecular Research (CCBR), University of Toronto, Toronto, Ontario, Canada, InDanio Bioscience Inc., Toronto, Ontario, Canada

[6] Department of Pathology and Molecular Medicine, Queen's University, Kingston, ON, Canada.

Running Title: Fungal derived 15-keto-prostaglandin E_2 and PPAR-γ promote *C. neoformans* infection

*Author for correspondence: Simon A. Johnston

Email: s.a.johnston@sheffield.ac.uk

Phone: +44 114 222 2301

Abstract

Cryptococcus neoformans is one of the leading causes of invasive fungal infection in humans worldwide. *C. neoformans* can use macrophages as a proliferative niche to increase infective burden and avoid immune surveillance. However, the specific mechanisms by which *C. neoformans* manipulates host immunity to promote its growth during infection remain ill-defined. Here we demonstrate that eicosanoid lipid mediators produced by *C. neoformans* play a key role in regulating pathogenesis. *C. neoformans* is known to secrete several eicosanoids that are highly similar to those found in vertebrate hosts. Using eicosanoid deficient cryptococcal mutants *Δplb1* and *Δlac1*, we demonstrate that prostaglandin E_2 is required by *C. neoformans* for proliferation within macrophages and, using our zebrafish model of cryptococcosis, we confirm this role for PGE_2 *in vivo*. We subsequently show that PGE_2 must be dehydrogenated into 15-keto-PGE_2 to promote fungal growth and that the mechanism of 15-keto-PGE_2 mediated virulence is via activation of the host receptor PPAR-γ.

Author Summary:

Cryptococcus neoformans is an opportunistic fungal pathogen that is responsible for significant numbers of deaths in the immunocompromised population worldwide. Here we address whether eicosanoids produced by *C. neoformans* manipulate host innate immune cells during infection. *Cryptococcus neoformans* produces several eicosanoids that are notable for their similarity to vertebrate eicosanoids, it is therefore possible that fungal-derived eicosanoids may provoke physiological effects in the host. Using a combination of *in vitro* and *in vivo* infection models we identify a specific eicosanoid species - prostaglandin E_2 – that is required by *C. neoformans* for growth during infection. We subsequently show that prostaglandin E_2 must be converted to 15-keto-prostaglandin E_2 within the host before it has these effects. Furthermore, we provide evidence that the mechanism of prostaglandin E_2/15-keto-prostaglandin E_2 mediated virulence

is via activation of host PPAR-γ – an intracellular eicosanoid receptor known to interact with 15-keto-PGE_2.

Introduction

Cryptococcus neoformans is an opportunistic pathogen that infects individuals who have severe immunodeficiencies, such as late-stage HIV infection. *C. neoformans* is estimated to infect 278,000 individuals each year resulting in 181,000 deaths (1,2). *C. neoformans* infection begins in the lungs and in the absence of an effective immune response the fungus disseminates to the central nervous system causing meningoencephalitis, and eventually death (3,4). In normal immunity, following phagocytosis of cryptococci, macrophages must become activated by further inflammatory signals from the host immune system before they can effectively kill *C. neoformans* (5,6). When this does not occur macrophages cannot kill *C. neoformans;* instead the fungus is able to proliferate rapidly intracellularly and may use macrophages to disseminate to the central nervous system where it causes fatal meningitis (7-11).

Eicosanoids are an important group of inflammatory mediators produced during the initial stages of microbial infection by innate immune cells such as macrophages. This diverse group of potent lipid signalling molecules have a short range of action and signal through autocrine and paracrine routes. During infection, macrophages produce large amounts of a particular group of eicosanoids called prostaglandins (12,13). Prostaglandins have a number of physiological effects throughout the body, but in the context of immunity they are known to strongly influence the inflammatory state (14). The prostaglandins PGE_2 and PGD_2 are the best-studied eicosanoid inflammatory mediators. During infection, macrophages produce both PGE_2 and PGD_2 to which, via autocrine routes, they are highly responsive (14). In vertebrate immunity, the synthesis of eicosanoids such as PGE_2 is carefully regulated by feedback loops to ensure that the potent effects of these molecules are properly constrained. Exogenous sources of eicosanoids within the body, such as from eicosanoid-producing parasites (15) or tumours that overproduce eicosanoids (16,17), can disrupt host inflammatory signaling as they are not subject to the same regulation.

During infection, *C. neoformans* produces a range of eicosanoid species which are indistinguishable from those produced by their vertebrate hosts (18-20). Currently only two *C. neoformans* enzymes - phospholipase B1 and laccase - are known to be associated with cryptococcal eicosanoid synthesis (20,21). Deletion of phospholipase B1 reduces secreted levels of all eicosanoids produced by *C. neoformans* suggesting that it has high level role in eicosanoid synthesis (21), perhaps fulfilling the role of phospholipase A_2 in higher organisms. In contrast, it is possible that the cryptococcal enzyme laccase has putative PGE_2 synthase activity (20). The synthesis of eicosanoids by *C. neoformans* raises the possibility that the fungus is able to manipulate the host inflammatory state by directly manipulating host eicosanoid signaling during the establishment of infection. It has previously been reported that the inhibition of prostaglandin E_2 receptors EP2 and EP4 during murine pulmonary infection leads to better host survival accompanied by a shift towards Th1/M1 macrophage activation, however it was not determined if PGE_2 was derived from the host or the fungus (22). Therefore, a key aspect of *C. neoformans* pathogenesis remains unanswered: do eicosanoids produced by *C. neoformans* manipulate host innate immune cells function during infection?

We have previously shown that the phospholipase B1 deficient strain *Δplb1,* that lacks eicosanoid synthesis, has reduced proliferation and survive within macrophages (23). We therefore hypothesised that eicosanoids produced by *C. neoformans* were able to promote intracellular proliferation within macrophages, and virulence in the host. To address this hypothesis, we combined *in vitro* macrophage infection assays with our previous published *in vivo* zebrafish model of cryptococcosis (24). Using this approach, we show that prostaglandin E_2 is sufficient to promote growth of *Δplb1* and *Δlac1* during *in vitro* infection of macrophages and furthermore that the source of PGE_2 during infection is from *C. neoformans* itself. We subsequently confirm that PGE_2 also promotes *C. neoformans* growth *in vivo* and that the biological effects of PGE_2 are mediated by its dehydrogenated form 15-keto-PGE_2. Finally, we determine that 15-keto-PGE_2 promotes *C. neoformans* infection via the activation of the host nuclear transcription factor PPAR-γ within infected macrophages.

Results

Prostaglandin E_2 is required for C. neoformans growth in macrophages

A previous study has identified PGE_2 as an eicosanoid that promotes cryptococcal virulence and manipulates macrophage activation, however this study did not determine if PGE_2 was produced by the host or *C. neoformans* (22). We have previously shown that the *C. neoformans PLB1* gene (coding for the secreted enzyme phospholipase B1) deletion mutant *Δplb1* (25) has impaired proliferation and survival during *in vitro* infection of J774 murine macrophage like cells (23). It has been proposed that the attenuation of *Δplb1* within macrophages could be because this strain cannot produce eicosanoids (21). To determine if PGE_2 promotes the intracellular growth of *C. neoformans* we treated *Δplb1* infected J774 cells with exogenous PGE_2 and measured intracellular proliferation over 18 hours. We found that the addition of exogenous PGE_2 to *Δplb1* infected J774 macrophages was sufficient to recover the intracellular proliferation of *Δplb1* compared to its H99 (parental wild type strain) and *Δplb1:PLB1* (reconstituted strain) (Fig 1A iii p= 0.038). We have previously described that the *Δplb1* has reduced intracellular proliferation due to a combination of reduced cell division and reduced viability within the phagosome (23) but in this case viability assays showed that exogenous PGE_2 produced no significant increase in the viability of *Δplb1* cells within the phagosome (Supplementary Figure 1A). These findings support our initial hypothesis and identify PGE_2 as a mediator of cryptococcal virulence during macrophage infection.

Phospholipase B1 dependent factors are sufficient to support Δplb1 growth in macrophages

To determine if *C. neoformans* is the source of PGE_2 during macrophage infection we used a co-infection assay which has previously been used to investigate the interaction of different *C. gattii* strains within the same macrophage (26). To produce co-infection, J774 murine macrophages were infected with a 50:50 mixture of *Δplb1* and H99-GFP (27) (Fig 1B i; as described previously for *C. gattii* (26)). If the parental strain H99 produces growth promoting eicosanoids that *Δplb1* cannot, the *Δplb1* strain should display improved intracellular replication when H99 is also present within the same macrophage. The intracellular proliferation of *Δplb1* was calculated by counting the change in number of non-fluorescent *Δplb1* cells over an 18hr period from time-lapse movies of infected cells. We found that co-infected macrophages did not always contain an equal ratio of each strain at the start of the 18hr period so we scored the proliferation of *Δplb1* for a range of initial burdens (1:2, 1:3 and 1:4). We found that *Δplb1* proliferated better when accompanied by two H99-GFP yeast cells in the same macrophage (Fig 1B ii, 1:2 $p = 0.014$) as opposed to when two *Δplb1* yeast cells were accompanied by one H99-GFP yeast cell (Fig 1B ii, 2:1). We observed a similar effect for ratios of 1:3 and 1:4, but these starting burden ratios are particularly rare, under powering our analysis (Supplementary Fig 1B). These data indicate that a phospholipase B1 dependent factor found in H99 infected macrophages, but absent in *Δplb1* infected macrophages, can support intracellular proliferation within macrophages.

Intracellular Cryptococcus neoformans infection does not lead to increased macrophage secretion of PGE$_2$

Our data indicate that the secreted factor identified during co-infection might be PGE$_2$ (Fig 1A, Fig 1B). It has been shown previously that the *Δplb1* mutant produces lower levels of eicosanoids (21) and *C. neoformans* infection can induce higher PGE$_2$ levels in the lung during *in vivo* pulmonary infection of mice (22). We thought that it might therefore be possible to detect a difference in PGE$_2$ levels between infected and uninfected macrophages as a result of cryptococcal eicosanoid synthesis. To test this, we performed ELISA analysis to detect PGE$_2$ concentrations in supernatants from *C. neoformans* infected J774 macrophages (Fig 1C). We found that J774 macrophages did produce detectable levels of PGE$_2$ (mean concentration 4.10 ng/1x10^6 cells), however we did not see any significant difference between infected or uninfected macrophages or between H99, *Δplb1* and *Δplb1:PLB1* infected cells. To confirm this, we performed LC MS/MS analysis of infected J774 macrophages using a PGE$_2$ standard for accurate quantification (Fig 1D). The concentrations detected were similar to those measured by our ELISA (mean concentration 6.35 ng/1X10^6 cells) and also did not show any significant differences between conditions. This suggests any *Cryptococcus*-derived eicosanoids present during infection are likely to be contained within the macrophage and that the host receptor targeted by these eicosanoids is therefore likely to be intracellular.

PGE$_2$ synthesis by C. neoformans is required for growth in vivo.

To confirm that *C. neoformans*-derived PGE$_2$ promotes fungal growth we used an *in vivo* model of cryptococcosis. Zebrafish have proven to be an excellent model for understanding vertebrate eicosanoid biology (28,29). One of the advantages of this infection model is that the fungal burden can be non-invasively imaged within infected larvae throughout infection by using fluorescently tagged *C. neoformans* strains. We therefore generated a constitutively expressed GFP tagged version of the *Δplb1* (*Δplb1*-GFP) for infection of zebrafish larvae. To evaluate the growth of *Δplb1*-GFP during infection of zebrafish larvae we injected 2 day post fertilisation (dpf) zebrafish larvae with *Δplb1*-GFP and measured the growth of the fungus at 1, 2 and 3 days post-infection (dpi). Analysis of fungal burden revealed that *Δplb1*-GFP had a lower fungal burden at 1, 2 and 3 days post infection (Fig 2D and supplementary figure 2A) compared to the parental strain H99-GFP (Fig 2A and supplementary figure 2A). These data show that the *Δplb1*-GFP mutant has a similar growth deficiency to our *in vitro* phenotype and agree with previous studies (23,25,30).

Our *in vitro* data suggest that *C. neoformans* is a source of virulence-enhancing eicosanoids during infection (Fig 1B). To investigate this *in vivo* we infected 2 dpf zebrafish larvae with H99-GFP and *Δplb1*-GFP as before but treated infected larvae with inhibitors for cyclooxygenase (COX) 1 and 2 - NS-398 (15 μM) and SC-560 (15 μM) respectively. Interestingly, we found that these inhibitors decreased the fungal burden within H99-GFP, but not *Δplb1*-GFP infected zebrafish larvae (Supplementary figure 2B and 2C, H99-GFP - NS-398, p= 0.0002, 1.85-fold decrease vs. DMSO. SC-560 p= <0.0001, 3.14-fold decrease vs DMSO). The intention of this treatment was to block host eicosanoid synthesis (28) however our data suggest that these inhibitors also block *C. neoformans* eicosanoid synthesis, which appears to have a greater effect on the outcome of infection. This phospholipase B1 dependent phenotype supports our previous evidence that *C. neoformans* is the source of eicosanoids during infection as these COX inhibitors produce a phenotype in H99-GFP infected larvae (eicosanoid producing) but not in *Δplb1*-GFP infected larvae (eicosanoid deficient).

Exogenous PGE_2 treatment partially rescues in vivo growth of Δplb1-GFP

To confirm that PGE_2 can promote infection *in vivo* we treated *Δplb1*-GFP and H99-GFP infected zebrafish larvae with PGE_2 and quantified its influence on fungal burden. In agreement with our *in vitro* findings, PGE_2 treatment increased the growth of both the parental H99 strain (Fig 2B, p = 0.0137, 1.35-fold increase vs. DMSO) and the *Δplb1*-GFP mutant (Fig 2E, p= 0.0001, 2.15-fold increase vs. DMSO) while PGD_2 did not (Fig 2C and 2F). Taken together these data show that the virulence of *C. neoformans in vivo* is enhanced by $PGE_{2,}$ furthermore our *in vitro* data suggest that this is a result of uncontrolled intracellular proliferation within macrophages (Fig 1).

Prostaglandin E_2 must be dehydrogenated into 15-keto-PGE_2 to promote C. neoformans growth. PGE_2 produced by *C. neoformans* can be further converted into 15-keto-PGE_2 (20). We reasoned that some of the PGE_2 added to zebrafish might be converted to 15-keto-PGE_2 which could have different biological activities to PGE_2. To explore this possibility we treated infected larvae with 16,16-dimethyl PGE_2, which cannot be dehydrogenated into 15-keto-PGE_2, but otherwise has comparable activity to PGE_2 (31). Interestingly, in contrast to PGE_2, we found that 16,16-dimethyl PGE_2 treatment did not increase the fungal burden of *Δplb1*-GFP (Fig 3C p= 0.9782) *or* H99-GFP infected larvae (Fig 3A p= 0.9954). This indicates that 15-keto-PGE_2 rather than PGE_2 is responsible for our previous observations (Fig 2B and 2E). To confirm the activity 15-keto-PGE_2 we treated infected larvae with exogenous 15-keto-PGE_2 and found that this was sufficient to significantly increase the fungal burden of both *Δplb1*-GFP (Fig 3D, p = 0.0119, 1.56-fold increase vs. DMSO) and H99-GFP infections (Fig 3B, p = 0.0048, 1.36-fold increase vs. DMSO). Taken together, these results demonstrate that the increase in *C. neoformans* burden observed with PGE_2 treatment is due to dehydrogenation of PGE_2 into 15-keto-PGE_2.

Prostaglandin E_2 is known to affect haematopoietic stem cell homeostasis in zebrafish (29) which could affect macrophage number and subsequently fungal burden. We have previously described that a large depletion of macrophages can lead to increased fungal burden in zebrafish larvae (24), however a near total reduction is required – up to 90% - because even at 24 hr only a small number of macrophages have phagocytosed the fungus meaning there is a large amount of redundant phagocytic capacity in the larvae. We performed whole body macrophage counts on 2 dpf uninfected larvae treated with PGE_2 or 15-keto-PGE_2 2 days post treatment (the same time points used in our infection assay). Following PGE_2 and 15-keto PGE_2 treatment macrophages were still observable throughout the larvae. For PGE_2 treatment we saw on average a 15% reduction in macrophage number while 15-keto PGE_2 did not cause any decrease (Supplementary Fig 3A). Due to the fact that fungal burden increased during both PGE_2 and 15-keto PGE_2 treatments it is highly unlikely that this reduction could account for the increases in burden seen.

To confirm the observations made with *Δplb1* we used a second eicosanoid deficient *C. neoformans* mutant *Δlac1*. Whereas *Δplb1* is unable to produce any eicosanoid species *Δlac1* is deficient only in PGE_2 and 15-keto-PGE_2 (20). Using a *Δlac1*-GFP strain generated for this study we repeated the *in vitro* co-infection assay and observed similar results to *Δplb1* (Fig 4A). These data strongly support our conclusion that *Cryptococcus*-derived PGE_2 / 15-keto-PGE_2 are fungal virulence factors. We subsequently tested *Δlac1*-GFP in *vivo* and found that this strain also produced low fungal burden during *in vivo* zebrafish larvae infection (Fig 4B). As with *Δplb1*-GFP, this defect could be rescued with the addition of exogenous PGE_2 (Fig 4C), but not with 16,16-dm-PGE_2 (Fig 4D) or with 15-keto-PGE_2 (Fig 4E).

15-keto-PGE_2 promotes C. neoformans growth by activating host PPAR-γ

We next wanted to determine if 15-keto-PGE_2 could promote cryptococcal growth by interfering with host eicosanoid signalling pathways. 16,16-dimethyl PGE_2 signals through the same host receptors as PGE_2 so its lack of activity in our model strongly suggests different molecular pathways for 15-keto-PGE_2 and PGE_2. PGE_2 has four cellular receptors (EP1, EP2, EP3 and EP4) each of which elicit varying cellular responses. In a murine model of pulmonary cryptococcosis EP2 and EP4 have been identified as promoters of fungal virulence (22). However, we found that treating H99-GFP infected zebrafish larvae with EP2/EP4 prostaglandin receptor antagonists had no effect on infection (Supplementary Fig 3B). 15-keto-PGE_2 has been reported as an agonist at the peroxisome proliferation associated receptor gamma (PPAR-γ) (32); a transcription factor that controls expression of many inflammation related genes (33-35). To determine if 15-keto-PGE_2 promotes the growth of *C. neoformans* during host infection by activating host PPAR-γ we treated infected larvae with a specific agonist of PPAR-γ - Troglitazone (TLT) - at a concentration (0.55 µM) previously shown to strongly activate PPAR-γ in zebrafish larvae (36). We found that TLT treatment significantly increased the fungal burden of *Δplb1*-GFP (Fig 5B and, p = 0.0089, 1.68-fold increase vs. DMSO), H99-GFP (Fig 5A, p = 0.0044, 1.46-fold increase vs. DMSO) and *Δlac1*-GFP (Fig 5C, p = 0.01, 1.94-fold increase vs. DMSO) infected larvae similar to 15-keto-PGE_2 treatment. These findings suggest that activating host PPAR-γ is sufficient to promote fungal growth.

Due to the extensive host/pathogen interactions between *C. neoformans* and host macrophages during infection, and the anti-inflammatory effects that PPAR-γ activation can have on macrophages, we hypothesised that PPAR-γ activation promoted intracellular proliferation within macrophages. To test this hypothesis, we treated H99 and *Δplb1* infected J774 murine macrophages with the PPAR-γ antagonist GW9662. In agreement with our hypothesis, GW9662 treatment significantly reduced the proliferation of H99, but not *Δplb1* (Fig 5D, p=0.026, 1.22-fold decrease vs. DMSO). These data suggest that PPAR-γ activation is necessary for the successful intracellular parasitism of host macrophages by *C. neoformans*. Furthermore, this must be due to eicosanoids produced by the fungus because *Δplb1* does not show a similar phenotype.

To confirm the 15-keto-PGE_2 activates PPAR-γ we treated 2 dpf zebrafish larvae from a PPAR-γ reporter fish line with 15-keto-PGE_2 and TLT (36). These fish have a GFP reporter for PPAR-γ that is strongly activated by TLT treatment. In support of the hypothesis that 15-keto-PGE_2 is an agonist to PPAR-γ we found that 15-keto-PGE_2 can compete with TLT for binding to PPAR-γ - evidenced by the decreased fluorescence of the reporter fish compared to TLT alone (Fig 5F). This phenotype is indicative of 15-keto-PGE_2 being a partial agonist for PPAR-γ (37,38). Finally, to confirm that 15-keto-PGE_2 mediated activation of PPAR-γ promotes cryptococcal virulence we treated *Δplb1*-GFP infected zebrafish larvae with exogenous 15-keto-PGE_2 as before but at the same time treated fish with the PPAR-γ antagonist GW9662 and found that, while 15-keto-PGE_2 treatment improved the growth of *Δplb1*-GFP during infection, the inhibition of PPAR-γ activation with GW9662 could specifically reverse this effect (Fig 5E).

Discussion

We have shown for the first time that eicosanoids produced by *C. neoformans* promote fungal virulence both *in vitro* and *in vivo*. In this respect we have shown that the intracellular growth defects of two eicosanoid deficient *C. neoformans* strains *Δplb1* and *Δlac1* (23,25) can be rescued with the addition of exogenous PGE_2. Furthermore, our *in vitro* co-infection and *in vivo* infection assays provide evidence that the source of this eicosanoid during infection is from the pathogen, rather than the host. Using an *in vivo* zebrafish larvae model of cryptococcosis we find that that PGE_2 must be dehydrogenated into 15-keto-PGE_2 before to influence fungal growth. Finally, we provide evidence that the mechanism of PGE_2/15-keto-PGE_2 mediated growth promotion during larval infection is via the activation of PPAR-γ – an intracellular receptor within macrophages that is known to promote an anti-inflammatory response (33,34,39-41).

In a previous study it was identified that the *C. neoformans* mutant *Δplb1* (that lacks the *PLB1* gene coding for phospholipase B1) was deficient in replication and survival in macrophages (23), a phenotype also observed by a number of studies using different *in vitro* infection assays (21,25). In this study we demonstrate that supplementing *Δplb1* with exogenous prostaglandin E_2 during macrophages infection is sufficient to restore the mutant's intracellular proliferation defect. To investigate whether the source of PGE_2 during infection might be *C. neoformans* we performed co-infection assays with H99 wild type cryptococci (eicosanoid producing) and *Δplb1* (eicosanoid deficient) within the same macrophage and found that co-infection was sufficient to promote the intracellular growth of *Δplb1*. We also observed similar interactions during *Δlac1* co-infection (a second eicosanoid deficient *C. neoformans* mutant). These observations agree with previous studies that suggest eicosanoids are virulence factors produced by *C. neoformans* during macrophage infection (21,42).

To determine if this secreted factor was PGE_2, we measured the levels of PGE_2 from *Cryptococcus* infected macrophages to see if there was an observable increase in this eicosanoid during infection. Although PGE_2 was detected, we did not see any significant difference between infected and uninfected macrophages, an observation confirmed using two different detection techniques – ELISA and LC MS/MS. These data suggest that PGE_2 produced by *C. neoformans* during macrophage infection is contained within the macrophage, likely in close proximity to the fungus and that the host receptor targeted by these eicosanoids is therefore likely to be intracellular.

A key goal of this study was to investigate how eicosanoids produced by *C. neoformans* modulate pathogenesis *in vivo* (24). To facilitate *in vivo* measurement of fungal burden we created two GFP-tagged strains with constitutive GFP expression - *Δplb1*-GFP and *Δlac1*-GFP - to use alongside the GFP-tagged H99 parental strain previously produced (27). These two mutants are the only *C. neoformans* mutants known to have a deficiency in eicosanoid synthesis. *Δplb1* cannot produce any eicosanoid species suggesting phospholipase B1 is high in the eicosanoid synthesis pathway while *Δlac1* has a specific defect in PGE_2 suggesting it might be a prostaglandin E_2 synthase enzyme. To our knowledge these are the first GFP tagged versions of *Δplb1* and *Δlac1* created. Characterisation of *Δplb1*-GFP and *Δlac1*-GFP *in vivo* revealed that both strains have significantly reduced fungal burdens compared to H99-GFP. This is the first report of *Δlac1* in zebrafish but these observations do confirm a previous zebrafish study showing that non-fluorescent *Δplb1* had attenuated infectious burden in zebrafish larvae (43).

Our *in vitro* co-infection experiments indicate that *C. neoformans* secretes virulence enhancing eicosanoids during infection. To confirm this *in vivo* we treated H99-GFP and *Δplb1*-GFP infected zebrafish larvae with COX-1 and COX-2 inhibitors and found that COX inhibition decreases fungal burden of H99-GFP but not *Δplb1*-GFP infected larvae. This phospholipase

B1 dependent phenotype supports our *in vitro* co-infection findings as it suggests that these COX inhibitors are affecting eicosanoid production by the fungus itself. The ability of COX inhibitors to inhibit eicosanoid production by *C. neoformans* is controversial (19,42) however our study is the first to use such selective COX inhibitors on *C. neoformans*.

To confirm that PGE_2 is required for cryptococcal growth *in vivo* we treated *Δplb1*-GFP and *Δlac1*-GFP infected zebrafish larvae with exogenous PGE_2 to determine how it would affect fungal burden. In agreement with our *in vitro* findings we found that PGE_2 significantly improved the growth of both of these strains within larvae. Interestingly we also found that PGE_2 improved the growth of H99-GFP, perhaps representing a wider manipulation of host immunity during *in vivo* infection.

In vertebrate cells, PGE_2 is converted into 15-keto-PGE_2 by the enzyme 15-prostaglandin dehydrogenase (15PGDH), furthermore it has been reported that *C. neoformans* has enzymatic activity analogous to 15PGDH (20). To investigate how the dehydrogenation of PGE_2 to 15-keto-PGE_2 influenced fungal burden we treated infected larvae with 16,16-dm-PGE_2 – a synthetic variant of PGE_2 which is resistant to dehydrogenation (31). Interestingly we found that 16,16-dm-PGE_2 was unable to promote the growth of *Δplb1*-GFP*,* H99-GFP or *Δlac1*-GFP within infected larvae. These findings indicate that 15-keto-PGE_2, rather than PGE_2, promotes cryptococcal virulence. We subsequently treated infected larvae with exogenous 15-keto-PGE_2 and confirmed that 15-keto-PGE_2 treatment was sufficient to promote the growth of both *Δplb1*-GFP and H99-GFP, but not *Δlac1*-GFP (discussed below), without the need for PGE_2. We therefore propose that PGE_2 produced by *C. neoformans* during infection must be enzymatically dehydrogenated into 15-keto-PGE_2 to promote cryptococcal virulence. These findings represent the identification of a new virulence factor (15-keto-PGE_2) produced by *C. neoformans,* as well as the first time identification of an eicosanoid other than PGE_2 with a role in promoting cryptococcal growth. Furthermore, our findings suggest that previous studies which identify

PGE_2 as a promoter of cryptococcal virulence (21,22,44) may have observed additive effects from both PGE_2 and 15-keto-PGE_2 activity.

The biological activity of 15-keto-PGE_2 is far less studied than PGE_2. It is known that 15-keto-PGE_2 cannot bind to prostaglandin E_2 EP receptors, this means it can act as a negative regulator of PGE_2 activity i.e. cells up-regulate 15PGDH activity to lower PGE_2 levels (45). Our findings however suggested that 15-keto-PGE_2 did have a biological activity independent of PGE_2 synthesis, possibly via a distinct eicosanoid receptor. It has been demonstrated that 15-keto-PGE_2 can activate the intracellular eicosanoid receptor peroxisome proliferator associated receptor gamma (PPAR- γ) (32). Activation of PPAR-γ by *C. neoformans* has not been described previously but it is compatible with what we know of cryptococcal pathogenesis. PPAR-γ is a nuclear receptor normally found within the cytosol. Upon ligand binding PPAR-γ forms a heterodimer with Retinoid X receptor (RXR) and translocates to the nucleus where it influences the expression of target genes which possess a peroxisome proliferation hormone response element (PPRE) (46). If eicosanoids are produced by *C. neoformans* during intracellular infection, it is likely that they bind to an intracellular eicosanoid receptor. Additionally, activation of PPAR-γ within macrophages is known to promote the expression of anti-inflammatory genes which could make the macrophage more amenable to parasitism by the fungus.

To investigate whether PPAR- γ activation could promote the growth of *C. neoformans* we treated *C. neoformans* infected zebrafish larvae with troglitazone (a specific PPAR-γ agonist). We used troglitazone at a concentration that is known to activate PPAR-γ (47) and confirmed that troglitazone was able to increase the growth of *Δplb1*-GFP*, Δlac1*-GFP and H99-GFP during infection.

Our experiments with the *Δlac1*-GFP strain reveals that this strain appears to respond in a similar way to PGE_2, 16,16-dm-PGE_2 and troglitazone as *Δplb1*-GFP but appears to be unresponsive to 15-keto-PGE_2. At this time, we cannot fully explain this phenotype, *Δlac1*-GFP was generally less responsive to PGE_2 and troglitazone treatments compared to *Δplb1*-GFP so it is possible that that higher concentrations of 15-keto-PGE_2 would be needed to rescue its growth defect, however experimentation with higher concentrations of 15-keto-PGE_2 led to significant host toxicity. The unresponsiveness of *Δlac1* to eicosanoid treatment could be due to unrelated virulence defects caused by laccase deficiency. Cryptococcal laccase expression is required for the production of fungal melanin – a well characterized virulence factor produced by *C. neoformans* (48,49). It is therefore possible that virulence defects unrelated to eicosanoid synthesis are preventing correct rescuing of this strain within our model.

After ascertaining that pharmacological activation of PPAR-γ promoted *C. neoformans* virulence we demonstrated that 15-keto-PGE_2 mediates its effects via the same pathway. In this respect, we found that the *in vitro* intracellular proliferation of the wild type H99 cryptococcal strain within J774 macrophages could be suppressed using a PPAR-γ antagonist GW9662. Furthermore, we found that treating *Δplb1*-GFP infected zebrafish larvae with GW9662 at the same time as 15-keto-PGE_2 blocked the virulence enhancing effects of the eicosanoid. These experiments show that 15-keto-PGE_2 mediates its effects through PPAR-γ. Finally, to confirm that 15-keto-PGE_2 is an agonist to PPAR-γ we performed experiments with zebrafish larvae from PPAR-γ GFP reporter fish (36) to demonstrate that that 15-keto-PGE_2 competes with troglitazone for binding to the PPAR-γ receptor *in vivo*. Taken together these experiments provide convincing evidence that a novel cryptococcal virulence factor - 15-keto-PGE_2 – enhances the virulence of *C. neoformans* by activation of host PPAR-γ and that macrophages are one of the key targets of this eicosanoid during infection.

In this study, we have shown for the first time that eicosanoids produced by *C. neoformans* can promote virulence in an *in vivo* host. Furthermore, we have provided evidence that this virulence occurs via eicosanoid mediated manipulation of host macrophages. We have identified that the eicosanoid responsible for these effects is 15-keto-PGE_2 which is derived from the dehydrogenation of PGE_2 produced by *C. neoformans*. We have subsequently demonstrated that 15-keto-PGE_2 mediates its effects via activation of PPAR- γ, an intracellular eicosanoid receptor known to promote anti-inflammatory immune pathways within macrophages. We provide compelling evidence that eicosanoids produced by *C. neoformans* enhance virulence, identifies a novel virulence factor – 15-keto-PGE_2 – and describes a novel mechanism of host manipulation by *C. neoformans* - activation of PPAR- γ. Most importantly this study provides a potential new therapeutic pathway for treatment of cryptococcal infection, as several eicosanoid modulating drugs are approved for patient treatment (50) .

Materials and methods

(all reagents are from Sigma-Aldrich, UK unless otherwise stated)

Ethics statement

Animal work was performed following UK law: Animal (Scientific Procedures) Act 1986, under Project License PPL 40/3574 and P1A4A7A5E. Ethical approval was granted by the University of Sheffield Local Ethical Review Panel. Experiments using the PPAR-γ reporter fish line (47) were conducted at the University of Toronto following approved animal protocols (# 00000698 “A live zebrafish-based screening system for human nuclear receptor ligand and cofactor discovery”) under a OMAFRA certificate.

Zebrafish

The following zebrafish strains were used for this study: *Nacre* wild type strain, *Tg(mpeg1:mCherryCAAX)sh378)* transgenic strain and the double mutant *casper*, for PPARγ reporter experiments (47), which lacks all melanophores and iridophores (51). Zebrafish were maintained according to standard protocols. Adult fish were maintained on a 14:10 – hour light / dark cycle at 28 ^{o}C in UK Home Office approved facilities in the Bateson Centre aquaria at the University of Sheffield.

C. neoformans

The H99-GFP strain has been previously described (27). The Δ*plb1*-GFP and Δ*lac1*-GFP stains was generated for this study by transforming existing deletion mutant strains (25,52) with a GFP expression construct (see below for transformation protocol). All strains used are in the *C. neoformans* variety *grubii* H99 genetic background.

Cryptococcus strains were grown for 18 hours at 28 ^{o}C, rotating horizontally at 20 rpm. *Cryptococcus* cultures were pelleted at 3300g for 1 minute, washed twice with PBS (Oxoidm Basingstoke, UK) and re-suspended in 1ml PBS. Washed cells were then counted with a haemocytometer and used as described below.

C. neoformans transformation

C. neoformans strains Δ*plb1* and Δ*lac1* were biolistically transformed using the pAG32_GFP transformation construct as previously described for H99-GFP (27). Stable transformants were identified by passaging positive GFP fluorescent colonies for at least 3 passages on YPD agar supplemented with 250 µg/ml Hygromycin B.

J774 Macrophage infection – with exogenous PGE$_2$ treatment

J774 macrophage (J774 cells were obtained from the ATCC, American Type Culture Collection) infection was performed as previously described (23) with the following alterations. J774 murine macrophage-like cells were cultured for a minimum of 4 passages in T75 tissue culture flasks at 37^{o}C 5% CO_2 in DMEM (High glucose, Sigma) supplemented with 10% Fetal Bovine Calf Serum (Invitrogen), 1% 10,000 units Penicillin / 10 mg streptomycin and 1 % 200 mM L – glutamine, fully confluent cells were used for each experiment. Macrophages were counted by haemocytometer and diluted to a concentration of $1x10^5$ cells per ml in DMEM supplemented with 1 µg/ml lipopolysaccharide (LPS from *E. coli,* Sigma L2630) before being plated into 24 well microplates (Greiner) and incubated for 24 hours (37 ^{o}C 5% CO_2).

Following 24-hour incubation, medium was removed and replaced with 1 ml DMEM supplemented with 2 nM prostaglandin E_2 (CAY14010, 1mg/ml stock in 100% ethanol). Macrophage wells were then infected with 100 µl $1x10^6$ yeast/ml *Cryptococcus* cells (from overnight culture, washed. See above) opsonized with anti-capsular IgG monoclonal antibody (18b7, a kind gift from Arturo Casadevall). Cells were incubated for 2 hours (37 ^{o}C 5% CO_2) and then washed with 37 ^{o}C PBS until extracellular yeast were removed. After washing, infected cells were treated with 1ml DMEM supplemented with PGE_2.

To calculate IPR, replicate wells for each treatment/strain were counted at 0 and 18 hours. Each well was washed once with 1ml 37 ^{o}C PBS prior to counting to remove any *Cryptococcus* cells released by macrophage death or vomocytosis. Intra-macrophage Cryptococci were released by lysis with 200 µl dH_2O for 20 minutes (lysis confirmed under microscope). Lysate was removed to a clean microcentrifuge tube and an additional 200 µl was used to wash the well to make a total lysate volume of 400 µl. *Cryptoccoccus* cells within lysates were counted by haemocytometer. IPR was calculated by dividing the total number of counted yeast at 18hr by the total at 0hr.

To assess the viability of *C. neoformans* cells recovered from macrophages we used our previously published colony forming unit (CFU) viability assay (23). Lysates from *C. neoformans* infected J774 cells were prepared from cells at 0hr and 18hr time points. The concentration of *C. neoformans* cells in the lysate was calculated by haemocytomter counting, the lysates were then diluted to give an expected concentration of $2x10^3$ yeast cells per ml. 100 µl of this diluted lysate was spread onto a YPD agar plate and incubated for 48 hr at 25^oC prior to colony counting.

J774 Macrophage co-infection.

J774 cells were prepared and seeded at a concentration of $1x10^5$ per ml as above in 24 well microplates and incubated for 24 hours (37 ^oC 5% CO_2), 45 minutes prior to infection J774 cells were activated with 150 ng/ml phorbol 12-myristate 13-acetate in DMSO added to 1 ml serum free DMEM. Following activation J774 cells were washed and infected with 100 µl / $1x10^6$ yeast/ml 50:50 mix of Δ*plb1* (non-fluorescent) and H99-GFP (e.g. $5x10^5$ Δ*plb1* and $5x10^5$ H99-GFP) or Δ*lac1-GFP* and H99 (non-fluorescent). Infected cells were incubated for 2 hours (37 ^oC 5% CO_2) to allow for phagocytosis of *Cryptococcus* and then washed multiple times with 37 ^oC PBS to remove unphagocytosed yeast, each well was observed between washes to ensure that macrophages were not being washed away. After washing 1 ml DMEM was added to each well.

Co-infected cells were imaged over 20 hours using a Nikon TE2000 microscope fitted with a climate controlled incubation chamber (37 ^oC 5% CO_2) using a Digital Sight DS-QiMC camera and a Plan APO Ph1 20x objective lens (Nikon). GFP and bright field images were captured every 4 minutes for 20 hours. Co-infection movies were scored manually. For example co-infected macrophages that contained 2 Δ*plb1* (non-fluorescent) and 1 H99-GFP (GFP positive) yeast cells at 0 hr were tracked for 18 hours and before the burden of each strain within the macrophage was counted again. The IPR for Δ*plb1* within co-infected macrophages was calculated by dividing the number of Δ*plb1* cells within a macrophage at 18 hr by the number at 0 hr.

Zebrafish infection

Washed and counted *Cryptococcus* cells from overnight culture were pelleted at 3300g for 1 minute and re-suspended in 10% Polyvinylpyrrolidinone (PVP), 0.5% Phenol Red in PBS to give the required inoculum in 1 nl. This injection fluid was loaded into glass capillaries shaped with a needle puller for microinjection. Zebrafish larvae were injected at 2-days post fertilisation; the embryos were anesthetised by immersion in 0.168 mg/ml tricaine in E3 before being transferred onto microscope slides coated with 3% methyl cellulose in E3 for injection. Prepared larvae were injected with two 0.5 nl boluses of injection fluid by compressed air into the yolk sac circulation valley. Following injection, larvae were removed from the glass slide and transferred to E3 to recover from anaesthetic and then transferred to fresh E3 to remove residual methyl cellulose. Successfully infected larvae (displaying systemic infection throughout the body and no visible signs of damage resulting from injection) were sorted using a fluorescent stereomicroscope. Infected larvae were maintained at 28 ^{o}C.

Eicosanoid / receptor agonist treatment of infected zebrafish larvae

All compounds were purchased from Cayman Chemical. Compounds were resuspended in DMSO and stored at -20 ^{o}C until used. Prostaglandin E_2 (CAY14010, 10mg/ml stock), Prostaglandin D_2 (CAY12010, 10mg/ml stock), 16,16-dimethyl-PGE_2 (CAY14750, 10mg/ml stock), 15-keto-PGE_2 (CAY14720, 10mg/ml stock), troglitazone (CAY14720, 10mg/ml stock), GW9662 (CAY70785,1mg/ml stock), AH6809 (CAY14050, 1mg/ml stock), GW627368X (CAY10009162, 10mg/ml stock), NS-398 (CAY70590, 9.4mg/ml stock), SC-560 (CAY70340, 5.3mg/ml stock).

Treatment with exogenous compounds during larval infected was performed by adding compounds (or equivalent solvent) to fish water (E3) to achieve the desired concentration. Fish were immersed in compound supplemented E3 throughout the experiment from the time of injection.

Zebrafish fungal burden measurement

Individual infected zebrafish embryos were placed into single wells of a 96 well plate (VWR) with 200 ul or E3 (unsupplemented E3, or E3 supplemented with eicosanoids / drugs depending on the assay). Infected embryos were imaged at 0 days post infection (dpi), 1 dpi, 2 dpi and 3 dpi in their 96 well plates using a Nikon Ti-E with a CFI Plan Achromat UW 2X N.A 0.06 objective lens. Images were captured with a Neo sCMOS (Andor, Belfast, UK) and NIS Elements (Nikon, Richmond, UK). Images were exported from NIS Elements into Image J FIJI as monochrome tif files. Images were threshholded in FIJI using the 'moments' threshold preset and converted to binary images to remove all pixels in the image that did not correspond to the intensity of the fluorescently tagged *C. neoformans*. The outline of the embryo was traced using the 'polygon' ROI tool, avoiding autofluorescence from the yolk sac. The total number of pixels in the threshholded image were counted using the FIJI 'analyse particles' function, the 'total area' measurement from the 'summary' readout was used for the total number of GFP$^+$ pixels in each embryo.

PPAR- γ GFP reporter fish treatment

PPARγ embryos were collected from homozygous ligand trap fish (F18). Embryos were raised in a temperature-controlled water system under LD cycle at 28.5° C. in 0.5×E2 media in petri-dishes till 1 dpf. Any developmentally delayed (dead or unfertilized) embryos were removed. Chorions were removed enzymatically with Pronase (1mg/ml) and specimens were dispensed into 24 well plates (10 per well) in 0.5×E2 media. For embryos 1% DMSO was used as a vehicle control. Chemicals were stored in DMSO, diluted appropriately and added individually to 400 ul of 0.5×E2 media with 0.05 U/ml penicillin and 50 ng/ml streptomycin and vortexed intensively for

1 min. 0.5×E2 media was removed from all wells with embryos and the 400 ul chemical solutions were administered to different wells to embryos. For drug treatment embryos were pre-incubated for 1 hour with compounds and then heat induced (28→37° C.) for 30 min in a water bath. Embryos were incubated at 28°C for 18 h and then monitored using a fluorescent dissection scope (SteREO Lumar.V12 Carl Zeiss) at 2 dpf. For analyzing GFP fluorescent pattern, embryos were anesthetized with Tricaine (Sigma, Cat.# A-5040) and mounted in 2 % methyl cellulose.

Whole body macrophage counts

2 dpf transgenic zebrafish larvae which have fluorescently tagged macrophages due to an mCherry fluorescent protein driven by the macrophage specific gene marker mpeg1 (53) *Tg(mpeg1:mCherryCAAX)sh378)* (24) were treated with 10 µM PGE_2, 10 µM 15-keto-PGE_2 or an equivalent DMSO control for 2 days. Larvae were then anesthetized by immersion in 0.168 mg/ml tricaine in E3 and imaged using a Nikon Ti-E with a Nikon Plan APO 20x/ 0.75 DIC N2 objective lens, taking z stacks of the entire body with 15 µM z steps. Macrophage counts were made manually using ImageJ from maximum projections.

Eicosanoid measurement (ELISA)

J774 macrophages were seeded into 24 well plates at a concentration of $1x10^5$ per well and and incubated for 24 hours at 37 ^oC 5 % CO_2. J774 cells were infected with *C. neoformans* as described above, at the same MOI 1:10 and incubated for 18 hours with 1ml serum free DMEM. At 18 hours post infection the supernatant was removed for ELISA analysis. Supernatants were analysed as per the PGE_2 EIA ELISA kit instructions (Cayman Chemical).

Eicosanoid measurement (Mass spectrometry)

J774 macrophages were seeded into T25 tissue culture flasks at a concentration of 1.3x10^6 cells per flask and incubated for 24 hours at 37 ^oC 5 % CO_2. J774 cells were infected with *C. neoformans* as described above, at the same MOI 1:10 and incubated for 18 hours with 2 ml serum free DMEM. At 18 hours post infection infected cells were scraped from the flask with a cell scraper into the existing supernatant and immediately snap frozen in ethanol / dry ice slurry. All samples were stored at -80 ^oC before analysis.

Lipids and lipid standards were purchased from Cayman Chemical (Ann Arbor, Michigan). Deuterated standard Prostaglandin E_2-d_4 (PGE_2-d_4), ≥98% deuterated form. HPLC grade solvents were from Thermo Fisher Scientific (Hemel Hempstead, Hertfordshire UK).

Lipids were extracted by adding a solvent mixture (1 mol/L acetic acid, isopropyl alcohol, hexane (2:20:30, v/v/v)) to the sample at a ratio of 2.5 –1 ml sample, vortexing, and then adding 2.5 ml of hexane (54). Where quantitation was required, 2 ng PGE_2-d_4, was added to samples before extraction, as internal standard. After vortexing and centrifugation, lipids were recovered in the upper hexane layer. The samples were then re-extracted by addition of an equal volume of hexane. The combined hexane layers were dried and analyzed for Prostaglandin E_2 (PGE_2) using LC-MS/MS as below.

Lipid extracts were separated by reverse-phase HPLC using a ZORBAX RRHD Eclipse Plus 95Å C18, 2.1 x 150 mm, 1.8 µm column (Agilent Technologies, Cheshire, UK), kept in a column oven maintained at 45°C. Lipids were eluted with a mobile phase consisting of A, water-B-acetic acid of 95:5:0.01 (vol/vol/vol), and B, acetonitrile-methanol-acetic acid of 80:15:0.01 (vol/vol/vol), in a gradient starting at 30% B. After 1 min that was ramped to 35% over 3 min, 67.5% over 8.5 min and to 100% over 5 min. This was subsequently maintained at 100% B for 3.5 min and then at 30% B for 1.5 min, with a flow rate of 0.5 ml/min. Products were monitored by LC/MS/MS in negative ion mode, on a 6500 Q-Trap (Sciex, Cheshire, United Kingdom) using parent-todaughter transitions of *m/z* 351.2 → 271.2 (PGE_2), and *m/z* 355.2 → 275.2 for PGE_2-d_4. ESI-MS/MS conditions were: TEM 475 °C, GS1 60, GS2 60, CUR 35, IS -4500 V, dwell time 75 s, DP -60 V, EP -10 V, CE -25 V and CXP at -10 V. PGE_2 was quantified using standard curves generated by varying PGE_2 with a fixed amount of PGE_2-d_4.

Acknowledgments

We thank the Bateson Centre aquaria staff for their assistance with zebrafish husbandry and the Johnston, Renshaw and Elks labs for critical discussions. We also thank Arturo Casadevall (Johns Hopkins University, Maryland USA) for providing the 18b7 antibody.

(1) Brown GD, Denning DW, Gow NA, Levitz SM, Netea MG, White TC. Hidden killers: human fungal infections. Sci Transl Med 2012 Dec 19;4(165):165rv13.

(2) Rajasingham R, Smith RM, Park BJ, Jarvis JN, Govender NP, Chiller TM, et al. Global burden of disease of HIV-associated cryptococcal meningitis: an updated analysis. Lancet Infect Dis 2017 May 5.

(3) Ma H, May RC. Chapter 5 Virulence in Cryptococcus Species. In: Allen I. Laskin,Sima Sariaslani and Geoffrey M.Gadd, editor. : Academic Press; 2009. p. 131-190.

(4) Gibson JF, Johnston SA. Immunity to Cryptococcus neoformans and C. gattii during cryptococcosis. Fungal Genet Biol 2015 May;78:76-86.

(5) Kawakami K, Kohno S, Kadota J, Tohyama M, Teruya K, Kudeken N, et al. T cell-dependent activation of macrophages and enhancement of their phagocytic activity in the lungs of mice inoculated with heat-killed Cryptococcus neoformans: involvement of IFN-gamma and its protective effect against cryptococcal infection. Microbiol Immunol 1995;39(2):135-143.

(6) Voelz K, Lammas DA, May RC. Cytokine signaling regulates the outcome of intracellular macrophage parasitism by Cryptococcus neoformans. Infect Immun 2009 Aug;77(8):3450-3457.

(7) Leopold Wager CM, Hole CR, Wozniak KL, Olszewski MA, Wormley FL,Jr. STAT1 signaling is essential for protection against Cryptococcus neoformans infection in mice. J Immunol 2014 Oct 15;193(8):4060-4071.

(8) Chrétien F, Lortholary O, Kansau I, Neuville S, Gray F, Dromer F. Pathogenesis of cerebral Cryptococcus neoformans infection after fungemia. J Infect Dis 2002 Aug;186:522-530.

(9) Charlier C, Nielsen K, Daou S, Brigitte M, Chretien F, Dromer F. PMC2612285; Evidence of a role for monocytes in dissemination and brain invasion by Cryptococcus neoformans. Infect Immun 2009 Jan;77:120-127.

(10) Gilbert AS, Seoane PI, Sephton-Clark P, Bojarczuk A, Hotham R, Giurisato E, et al. Vomocytosis of live pathogens from macrophages is regulated by the atypical MAP kinase ERK5. Sci Adv 2017 08/16;3(8).

(11) Smith LM, Dixon EF, May RC. The fungal pathogen Cryptococcus neoformans manipulates macrophage phagosome maturation. Cell Microbiol 2015 May;17(5):702-713.

(12) Norris PC, Reichart D, Dumlao DS, Glass CK, Dennis EA. Specificity of eicosanoid production depends on the TLR-4-stimulated macrophage phenotype. J Leukoc Biol 2011 Sep;90(3):563-574.

(13) Gupta S, Maurya MR, Stephens DL, Dennis EA, Subramaniam S. An integrated model of eicosanoid metabolism and signaling based on lipidomics flux analysis. Biophys J 2009 Jun 3;96(11):4542-4551.

(14) Harizi H. The immunobiology of prostanoid receptor signaling in connecting innate and adaptive immunity. Biomed Res Int 2013;2013:683405.

(15) Angeli V, Faveeuw C, Roye O, Fontaine J, Teissier E, Capron A, et al. Role of the parasite-derived prostaglandin D2 in the inhibition of epidermal Langerhans cell migration during schistosomiasis infection. J Exp Med 2001 May 21;193(10):1135-1147.

(16) Ahmadi M, Emery DC, Morgan DJ. Prevention of both direct and cross-priming of antitumor CD8+ T-cell responses following overproduction of prostaglandin E2 by tumor cells in vivo. Cancer Res 2008 Sep 15;68(18):7520-7529.

(17) Harizi H, Corcuff JB, Gualde N. Arachidonic-acid-derived eicosanoids: roles in biology and immunopathology. Trends Mol Med 2008 Oct;14:461-469.

(18) Noverr MC, Erb-Downward JR, Huffnagle GB. Production of eicosanoids and other oxylipins by pathogenic eukaryotic microbes. Clin Microbiol Rev 2003 Jul;16(3):517-533.

(19) Erb-Downward JR, Huffnagle GB. Cryptococcus neoformans produces authentic prostaglandin E2 without a cyclooxygenase. Eukaryot Cell 2007 Feb;6(2):346-350.

(20) Erb-Downward JR, Noggle RM, Williamson PR, Huffnagle GB. The role of laccase in prostaglandin production by Cryptococcus neoformans. Mol Microbiol 2008 Jun;68(6):1428-1437.

(21) Noverr MC, Cox GM, Perfect JR, Huffnagle GB. PMC148814; Role of PLB1 in pulmonary inflammation and cryptococcal eicosanoid production. Infect Immun 2003 Mar;71:1538-1547.

(22) Shen L, Liu Y. Prostaglandin E2 blockade enhances the pulmonary anti-Cryptococcus neoformans immune reaction via the induction of TLR-4. Int Immunopharmacol 2015 Sep;28(1):376-381.

(23) Evans RJ, Li Z, Hughes WS, Djordjevic JT, Nielsen K, May RC. Cryptococcal Phospholipase B1 (Plb1) is required for intracellular proliferation and control of titan cell morphology during macrophage infection. Infect Immun 2015 Jan 20.

(24) Bojarczuk A, Miller KA, Hotham R, Lewis A, Ogryzko NV, Kamuyango AA, et al. Cryptococcus neoformans Intracellular Proliferation and Capsule Size Determines Early Macrophage Control of Infection. Sci Rep 2016 Feb 18;6:21489.

(25) Cox GM, McDade HC, Chen SC, Tucker SC, Gottfredsson M, Wright LC, et al. Extracellular phospholipase activity is a virulence factor for Cryptococcus neoformans. Mol Microbiol 2001 Jan;39:166-175.

(26) Voelz K, Johnston SA, Smith LM, Hall RA, Idnurm A, May RC. 'Division of labour' in response to host oxidative burst drives a fatal Cryptococcus gattii outbreak. Nat Commun 2014 Oct 17;5:5194.

(27) Voelz K, Johnston SA, Rutherford JC, May RC. Automated analysis of cryptococcal macrophage parasitism using GFP-tagged cryptococci. PLoS One 2010 Dec 31;5(12):e15968.

(28) Feng Y, Renshaw S, Martin P. Live imaging of tumor initiation in zebrafish larvae reveals a trophic role for leukocyte-derived PGE(2). Curr Biol 2012 Jul 10;22(13):1253-1259.

(29) North TE, Goessling W, Walkley CR, Lengerke C, Kopani KR, Lord AM, et al. Prostaglandin E2 regulates vertebrate haematopoietic stem cell homeostasis. Nature 2007 Jun 21;447(7147):1007-1011.

(30) Chayakulkeeree M, Johnston SA, Oei JB, Lev S, Williamson PR, Wilson CF, et al. SEC14 is a specific requirement for secretion of phospholipase B1 and pathogenicity of Cryptococcus neoformans. Mol Microbiol 2011 May;80:1088-1101.

(31) Ohno H, Morikawa Y, Hirata F. Studies on 15-hydroxyprostaglandin dehydrogenase with various prostaglandin analogues. J Biochem 1978 Dec;84(6):1485-1494.

(32) Chou WL, Chuang LM, Chou CC, Wang AH, Lawson JA, FitzGerald GA, et al. Identification of a novel prostaglandin reductase reveals the involvement of prostaglandin E2 catabolism in regulation of peroxisome proliferator-activated receptor gamma activation. J Biol Chem 2007 Jun 22;282(25):18162-18172.

(33) Alleva DG, Johnson EB, Lio FM, Boehme SA, Conlon PJ, Crowe PD. Regulation of murine macrophage proinflammatory and anti-inflammatory cytokines by ligands for peroxisome proliferator-activated receptor-gamma: counter-regulatory activity by IFN-gamma. J Leukoc Biol 2002 Apr;71(4):677-685.

(34) Maggi LB,Jr, Sadeghi H, Weigand C, Scarim AL, Heitmeier MR, Corbett JA. Anti-inflammatory actions of 15-deoxy-delta 12,14-prostaglandin J2 and troglitazone: evidence for heat shock-dependent and -independent inhibition of cytokine-induced inducible nitric oxide synthase expression. Diabetes 2000 Mar;49(3):346-355.

(35) Jiang C, Ting AT, Seed B. PPAR-gamma agonists inhibit production of monocyte inflammatory cytokines. Nature 1998 Jan;391:82-86.

(36) Tiefenbach J, Moll PR, Nelson MR, Hu C, Baev L, Kislinger T, et al. A live zebrafish-based screening system for human nuclear receptor ligand and cofactor discovery. PLoS One 2010 Mar 22;5(3):e9797.

(37) Atanasov AG, Wang JN, Gu SP, Bu J, Kramer MP, Baumgartner L, et al. Honokiol: a non-adipogenic PPARgamma agonist from nature. Biochim Biophys Acta 2013 Oct;1830(10):4813-4819.

(38) Bhalla K, Hwang BJ, Choi JH, Dewi R, Ou L, Mclenithan J, et al. N-Acetylfarnesylcysteine is a novel class of peroxisome proliferator-activated receptor gamma ligand with partial and full agonist activity in vitro and in vivo. J Biol Chem 2011 Dec 2;286(48):41626-41635.

(39) Bouhlel MA, Derudas B, Rigamonti E, Dievart R, Brozek J, Haulon S, et al. PPARgamma activation primes human monocytes into alternative M2 macrophages with anti-inflammatory properties. Cell Metab 2007 Aug;6(2):137-143.

(40) Bonfield TL, Thomassen MJ, Farver CF, Abraham S, Koloze MT, Zhang X, et al. Peroxisome proliferator-activated receptor-gamma regulates the expression of alveolar macrophage macrophage colony-stimulating factor. J Immunol 2008 Jul 1;181(1):235-242.

(41) Odegaard JI, Ricardo-Gonzalez RR, Goforth MH, Morel CR, Subramanian V, Mukundan L, et al. Macrophage-specific PPARgamma controls alternative activation and improves insulin resistance. Nature 2007 Jun 28;447(7148):1116-1120.

(42) Noverr MC, Phare SM, Toews GB, Coffey MJ, Huffnagle GB. Pathogenic yeasts Cryptococcus neoformans and Candida albicans produce immunomodulatory prostaglandins. Infect Immun 2001 May;69(5):2957-2963.

(43) Tenor JL, Oehlers SH, Yang JL, Tobin DM, Perfect JR. Live Imaging of Host-Parasite Interactions in a Zebrafish Infection Model Reveals Cryptococcal Determinants of Virulence and Central Nervous System Invasion. MBio 2015 Sep 29;6(5):e01425-15.

(44) Valdez PA, Vithayathil PJ, Janelsins BM, Shaffer AL, Williamson PR, Datta SK. Prostaglandin E2 suppresses antifungal immunity by inhibiting interferon regulatory factor 4 function and interleukin-17 expression in T cells. Immunity 2012 Apr 20;36(4):668-679.

(45) Coggins KG, Latour A, Nguyen MS, Audoly L, Coffman TM, Koller BH. Metabolism of PGE2 by prostaglandin dehydrogenase is essential for remodeling the ductus arteriosus. Nat Med 2002 Feb;8(2):91-92.

(46) Lemberger T, Desvergne B, Wahli W. Peroxisome proliferator-activated receptors: a nuclear receptor signaling pathway in lipid physiology. Annu Rev Cell Dev Biol 1996;12:335-363.

(47) Tiefenbach J, Moll PR, Nelson MR, Hu C, Baev L, Kislinger T, et al. A live zebrafish-based screening system for human nuclear receptor ligand and cofactor discovery. PLoS One 2010 Mar 22;5(3):e9797.

(48) Salas SD, Bennett JE, Kwon-Chung KJ, Perfect JR, Williamson PR. Effect of the laccase gene CNLAC1, on virulence of Cryptococcus neoformans. J Exp Med 1996 Aug 1;184(2):377-386.

(49) Qiu Y, Davis MJ, Dayrit JK, Hadd Z, Meister DL, Osterholzer JJ, et al. Immune modulation mediated by cryptococcal laccase promotes pulmonary growth and brain dissemination of virulent Cryptococcus neoformans in mice. PLoS One 2012;7(10):e47853.

(50) Day RO, Graham GG. Non-steroidal anti-inflammatory drugs (NSAIDs). BMJ 2013 Jun 11;346:f3195.

(51) White RM, Sessa A, Burke C, Bowman T, LeBlanc J, Ceol C, et al. Transparent adult zebrafish as a tool for in vivo transplantation analysis. Cell Stem Cell 2008 Feb 7;2(2):183-189.

(52) Zhu X, Williamson PR. Role of laccase in the biology and virulence of Cryptococcus neoformans. FEMS Yeast Res 2004 Oct;5(1):1-10.

(53) Ellett F, Pase L, Hayman JW, Andrianopoulos A, Lieschke GJ. Mpeg1 Promoter Transgenes Direct Macrophage-Lineage Expression in Zebrafish. Blood 2011 Jan 27;117(4):e49-56.

(54) Maskrey BH, Bermudez-Fajardo A, Morgan AH, Stewart-Jones E, Dioszeghy V, Taylor GW, et al. Activated platelets and monocytes generate four hydroxyphosphatidylethanolamines via lipoxygenase. J Biol Chem 2007 Jul 13;282(28):20151-20163.

Fig1

The intracellular proliferation defect of the *C.* neoformans mutant *Δplb1,* can be reversed with the addition of exogenous prostaglandin E_2. A J774 murine macrophages were infected with *Δplb1,* the parental strain H99 or a genetic reconstitute strain *Δplb1:PLB1* . Infected cells were left untreated **(i)** or treated with 2 nM PGE_2 or an equivalent solvent (ethanol) control **(ii, iii, iv)**. Mean IPR from 5 biological repeats shown with error bars representing standard deviation. An unpaired two tailed Student's t-test was performed to compare each treatment group. **(i) *** p = 0.0303 **(ii)** ns p = 0.7212 **(iii)** * p = 0.0376 **(iv)** ns p=0.723. **B** J774 cells co-infected with a 50:50 mix of *Δplb1* and H99-GFP. **i** Diagrammatic representation of co-infection experiment. GFP^+ (green) and GFP^- (yellow) *C. neoformans* cells within the phagosome were quantified at 0 hr, macrophages with a burden ratio of 1:2 or 2:1 were reanalysed at 18 hr, the IPR for *Δplb1* within 2:1 and 1:2 co-infected cells was calculated by dividing the burden at 18hr by burden at 0 hr for GFP^+ (green) or GFP^- (yellow) cells. **ii** Quantification of IPR for *Δplb1* cells within *Δplb1*:H99-GFP 2:1 or 1:2 co-infected macrophages. At least 35 co-infected macrophages were analysed for each condition over 4 experimental repeats. Student's T test performed to compare ratios – 2:1 vs 1:2 * p = 0.0137. **C** PGE_2 monoclonal EIA ELISA performed on supernatants from *C. neoformans* infected macrophages collected at 18 hr post infection. Mean concentration of PGE_2 (pg per $1x10^6$ cells) plotted with SD, n = 4. One-way ANOVA with Tukey post-test performed, no significance found. **D** LC MS/MS mass spectrometry analysis performed on cell suspensions (infected J774 cells and supernatants) collected at 18 hr post infection. Mean concentration of PGE_2 (pg per $1x10^6$ cells) plotted with SD, n = 3. One-way ANOVA with Tukey post-test performed, no significance found.

Fig2

The prostaglandin E_2 dependent growth defect of *Δplb1* is also present *in vivo*: A i H99-GFP infected larvae imaged at 0, 1, 2 and 3 dpi. At least 50 larvae measured per time point across 3 biological repeats. Box and whiskers show median, 5th percentile and 95th percentile. Unpaired Mann-Whitney U tests used to compare the burden between each strain for every time point, for p values see (Supplementary Fig1 A + B). **B i** – H99-GFP Infected larvae treated with 10 µM prostaglandin E_2 or equivalent solvent (DMSO) control. At least 60 larvae measured per treatment group from 3 biological repeats. Box and whiskers show median, 5th percentile and 95th percentile. Unpaired Mann-Whitney U tests used to compare between treatments DMSO vs. 10 µM PGE_2 * p = 0.0137 (threshold for significance 0.017, corrected for multiple comparisons). **C i,** H99-GFP Infected larvae treated with 10 µM prostaglandin D_2 or equivalent solvent (DMSO) control. At least 60 larvae measured per treatment group from 4 biological repeats. Box and whiskers show median, 5th percentile and 95th percentile. Unpaired Mann-Whitney U tests used to compare between treatments DMSO vs. 10 µM $PGD_{2.,}$ ns p= 0.8 **D i** *Δplb1*-GFP infected larvae (500 cell inoculum injected at 2 dpf) imaged at 0, 1, 2 and 3 dpi. N = 3. Box and whiskers show median, 5th percentile and 95th percentile. At least 87 larvae measured for each time point from 3 biological repeats. Unpaired Mann-Whitney U tests used to compare the burden between each strain for every time point, for p values see (Supplementary Fig 1). **E i** *Δplb1*-GFP Infected larvae treated with 10 µM prostaglandin E_2 or equivalent solvent (DMSO) control. At least 35 larvae measured per treatment group from 2 biological repeats. Box and whiskers show median, 5th percentile and 95th percentile. Unpaired Mann-Whitney U tests used to compare between treatments *Δplb1*-GFP DMSO vs 10 µM PGE_2 *** p = 0.0001 (threshold for significance 0.017, corrected for multiple comparisons). **F i** *Δplb1*-GFP Infected larvae treated with 10 µM prostaglandin D_2 or equivalent solvent (DMSO) control. At least 45 larvae measured per treatment group from 3 biological repeats. Box and whiskers show median, 5th percentile and 95th percentile. Unpaired Mann-Whitney U tests used to compare between treatments DMSO vs. 10 µM PGD_2. Ns p = 0.1 **A ii** Representative GFP images (representative = median value) H99-GFP infected larvae, untreated at 0,1,2,3 dpi. **B ii, C ii** Representative GFP images (representative = median value) H99-GFP infected larvae, at 2 dpi treated with 10 µM PGE_2 (**B ii**) or PGD_2 (**C ii**). **D ii** Representative GFP images (representative = median value) *Δplb1*-GFP infected larvae, untreated at 0,1,2,3 dpi. **E ii, F ii** Representative GFP images (representative = median value) *Δplb1*-GFP infected larvae, at 2 dpi treated with 10 µM PGE_2 (**E ii**) or PGD_2 (**F ii**).

Fig3

The observed activity of PGE_2 is due to its dehydrogenated derivative 15-keto-PGE_2: Fungal burden measured at 2 days post infection (2 dpi) by counting GFP positive pixels in each larvae. **A i** H99-GFP Infected larvae treated with 10 µM 16,16-dimethyl-prostaglandin E_2 or equivalent solvent (DMSO) control. At least 75 larvae measured per treatment group from 4 biological repeats. Box and whiskers show median, 5th percentile and 95th percentile. Unpaired Mann-Whitney U test used to compare between treatments, DMSO vs. 10 µM 16, 16-dm PGE_2 ns $p = 0.9954$. **B i** H99-GFP Infected larvae treated with 10 µM 15-keto-prostaglandin E_2 or equivalent solvent (DMSO) control. At least 55 larvae measured per treatment group from 3 biological repeats. Unpaired Mann-Whitney U test used to compare between treatments DMSO vs. 10 µM 15-keto=PGE_2 ** $p = 0.0048$ (threshold for significance 0.017, corrected for multiple comparisons). **C i** *Δplb1*-GFP Infected larvae treated with 10 µM 16, 16-dimethyl prostaglandin E_2 or equivalent solvent (DMSO) control. At least 45 larvae per treatment group from 3 biological repeats. Unpaired Mann-Whitney U test used to compare between treatments *Δplb1*-GFP DMSO vs 10 µM 16, 16-dm PGE_2 ns $p = 0.98$. **D i** *Δplb1*-GFP Infected larvae treated with 10 µM 15-keto-prostaglandin E_2 or equivalent solvent (DMSO) control. At least 35 larvae measured per treatment group from 2 biological repeats. Unpaired Mann-Whitney U test used to compare between treatments DMSO vs 10 µM 15-keto-PGE_2 * $p = 0.0119$ (threshold for significance 0.017, corrected for multiple comparisons). **A ii, B ii** Representative GFP images (representative = median value) H99-GFP infected larvae, at 2dpi treated with 10 µM 16,16-dm-PGE_2 (**A ii**) or 15-keto-PGE_2 (**B ii**). **Cii, D ii** Representative GFP images (representative = median value) *Δplb1*-GFP infected larvae, at 2dpi treated with 10 µM 16,16-dm-PGE_2 (**C ii**) or 15-keto-PGE_2 (**D ii**).

Fig4

A J774 cells co-infected with a 50:50 mix of *Δlac1*-GFP and H99. Quantification of IPR for *Δlac1*-GFP cells within *Δlac1*-GFP:H99 2:1 or 1:2 co-infected macrophages. At least 20 co-infected macrophages were analysed for each condition over 4 experimental repeats. Student's T test performed to compare ratios – 2:1 vs 1:2 * p = 0.012. **B i** *Δlac1*-GFP infected larvae imaged at 0, 1, 2 and 3 dpi. Fungal burden measured by counting GFP positive pixels in each larvae. At least 78 larvae measured per time point across 3 biological repeats. Box and whiskers show median, 5th percentile and 95th percentile. Unpaired Mann-Whitney U tests used to compare the burden between each strain for every time point, for p values see (Supplementary Fig2 A + B). **B ii** Representative GFP images (representative = median value) of 2dpi *Δlac1*-GFP infected larvae, untreated at 0,1,2,3 dpi **C i** *Δlac1*-GFP Infected larvae treated with 10 µM prostaglandin E_2 or equivalent solvent (DMSO) control. At least 70 larvae measured per treatment group across 4 biological repeats. Box and whiskers show median, 5th percentile and 95th percentile. Unpaired Mann-Whitney U test used to compare between treatments, DMSO vs. 10 µM PGE_2 * p = 0.035. **D i** *Δlac1*-GFP Infected larvae treated with 10 µM 16,16-dimethyl prostaglandin E_2 or equivalent solvent (DMSO) control. At least 75 larvae measured per treatment group across 4 biological repeats. Box and whiskers show median, 5th percentile and 95th percentile. Unpaired Mann-Whitney U test used to compare between treatments, DMSO vs. 10 µM 16,16-dimethyl prostaglandin E_2 ns p = 0.062. **E i** *Δlac1*-GFP Infected larvae treated with 10 µM 15-keto-prostaglandin E_2 or equivalent solvent (DMSO) control. At least 58 larvae measured per treatment group across 3 biological repeats. Unpaired Mann-Whitney U test used to compare between treatments DMSO vs. 10 µM 15-keto-prostaglandin E_2 ns p= 0.50. **C ii, D ii, E ii** Representative GFP images (representative = median value) *Δlac1*-GFP infected larvae, at 2 dpi treated with 10 µM PGE_2 (**C ii**), 16,16-dm-PGE_2 (**D ii**) or 15-keto-PGE_2 (**E ii**).

Fig5

15-keto-PGE$_2$ may promote fungal burden by activating host PPAR- γ. 2 day old (2 dpf) *Nacre* zebrafish larvae injected with 500 cell inoculum. Fungal burden measured at 2 days post infection (2 dpi) by counting GFP positive pixels within each larvae. **A i** H99-GFP Infected larvae treated with 0.55 µM Troglitazone (TLT) equivalent solvent (DMSO) control. Box and whiskers show median, 5th percentile and 95th percentile. At least 55 larvae measured per treatment group over 3 biological repeats. Mann-Whitney U test used to compare between treatments, DMSO vs. 0.55 µM Troglitazone ** p = 0.0044 (threshold for significance 0.025, corrected for multiple comparisons). **B i** *Δplb1*-GFP infected larvae treated with 0.55 µM Troglitazone (TLT) equivalent solvent (DMSO) control. Box and whiskers show median, 5th percentile and 95th percentile. At least 35 larvae measured per treatment group from 2 biological repeats. Mann-Whitney U test used to compare between treatments, DMSO vs. 0.55 µM Troglitazone ** p = 0.0089 (threshold for significance 0.025, corrected for multiple comparisons). **C i** *Δlac1*-GFP infected larvae treated with 0.55 µM Troglitazone (TLT) equivalent solvent (DMSO) control. At least 60 larvae measured per treatment group from 3 biological repeats. Box and whiskers show median, 5th percentile and 95th percentile, DMSO vs. 0.55 µM Troglitazone * p = 0.01 (threshold for significance 0.025, corrected for multiple comparisons). **A ii, B ii and Cii,** Representative GFP images (representative = median value) *C. neoformans* infected larvae, at 2 dpi treated with 0.55 µM Troglitazone (TLT) **A ii -** H99-GFP, **B ii -** *Δplb1*-GFP and **C ii** *Δlac1*-GFP. **D** J774 murine macrophages infected with *Δplb1* or the parental strain H99. Infected cells treated with 25 µM GW9662 (a PPAR-γ antagonist) or equivalent solvent (DMSO) control. Mean IPR from 6 biological repeats shown with error bars representing standard deviation. An unpaired two tailed Student's t-test was performed to compare each treatment group. H99 DMSO vs. H99 25 µM GW9662 * p = 0.026. **E** *Δplb1*-GFP infected larvae treated with 10 µM 15-keto-PGE$_2$, 500 nM GW9662, 10 µM 15-keto-PGE$_2$ + 500 nM GW9662 or an equivalent solvent

(DMSO) control. Box and whiskers show median, 5th percentile and 95th percentile. At least 35 larvae measured per treatment group from 2 biological repeats. Mann-Whitney U test used to compare between treatments. DMSO vs. 15-keto-PGE$_2$ **** $p < 0.0001$ (threshold for significance 0.025, corrected for multiple comparisons), 15-keto-PGE$_2$ vs. 15-keto-PGE$_2$ + 500 nm GW9662 ** $p = 0.005$ (threshold for significance 0.025, corrected for multiple comparisons) **F** Transgenic zebrafish larvae with a GFP PPAR- γ reporter treated with DMSO, 250 nM Troglitazone or 10 µM 15-keto-PGE$_2$ + 250 nM Troglitazone overnight and imaged. Lateral views of 2 dpf embryos, anterior to the left, are shown.

Supplementary Fig1

Quantification of IPR for *Δplb1* cells within *Δplb1*:H99-GFP co-infected macrophages at initial burdens of 2:1, 3:1, 4:1 and vice versa. N=4. Student's T test performed to compare ratios – 2:1 vs 1:2 * p = 0.0137.

Supplementary Figure 2

Comparison of fungal burden between H99-GFP and *Δplb1*-GFP infected larvae A (Data reproduced from Fig2 A and E for clarity) H99-GFP and *Δplb1*-GFP infected larvae imaged at 0, 1, 2 and 3 dpi. At least 50 larvae measured per time point from 3 biological repeats. Box and whiskers show median, 5th percentile and 95th percentile. Unpaired Mann-Whitney U tests used to compare the burden between each strain for every time point. **B** Results of Mann-Whitney U tests comparing burden between time points. **C i** H99-GFP infected larvae treated with 15 µM NS-398, 15 µM SC-560 or equivalent solvent (DMSO) control. Box and whiskers show median, 5th percentile and 95th percentile. At least 25 larvae measured per treatment group from 2 biological repeats. Mann-Whitney U test used to compare between treatments, DMSO vs. 15 µM *** p = 0.0002. **ii** *Δplb1*-GFP infected larvae treated with 15 µM NS-398, 15 µM SC-560 or equivalent solvent (DMSO) control. Box and whiskers show median, 5th percentile and 95th percentile. At least 34 larvae measured per treatment group from 2 biological repeats. Mann-Whitney U test used to compare between treatments, no significance found.

Supplementary figure 3

A Whole body macrophage counts of zebrafish larvae treated at 2 dpf with 10 µM PGE_2, 10 µM 15-keto-PGE_2 or an equivalent DMSO control for 2 days. Box and whiskers show median, 5th percentile and 95th percentile. At least 12 larvae measured per treatment group per biological repeat n = 4. Mann-Whitney U test used to treatments to DMSO control ** p = 0.0025. **B** H99-GFP infected larvae treated with a combination of 3 µM NS-398 and 3 µM SC-560 or equivalent solvent (DMSO) control. Box and whiskers show median, 5th percentile and 95th percentile. At least 64 larvae measured per treatment group from 4 biological repeats. Mann-Whitney U test used to compare between treatments, no significance found.

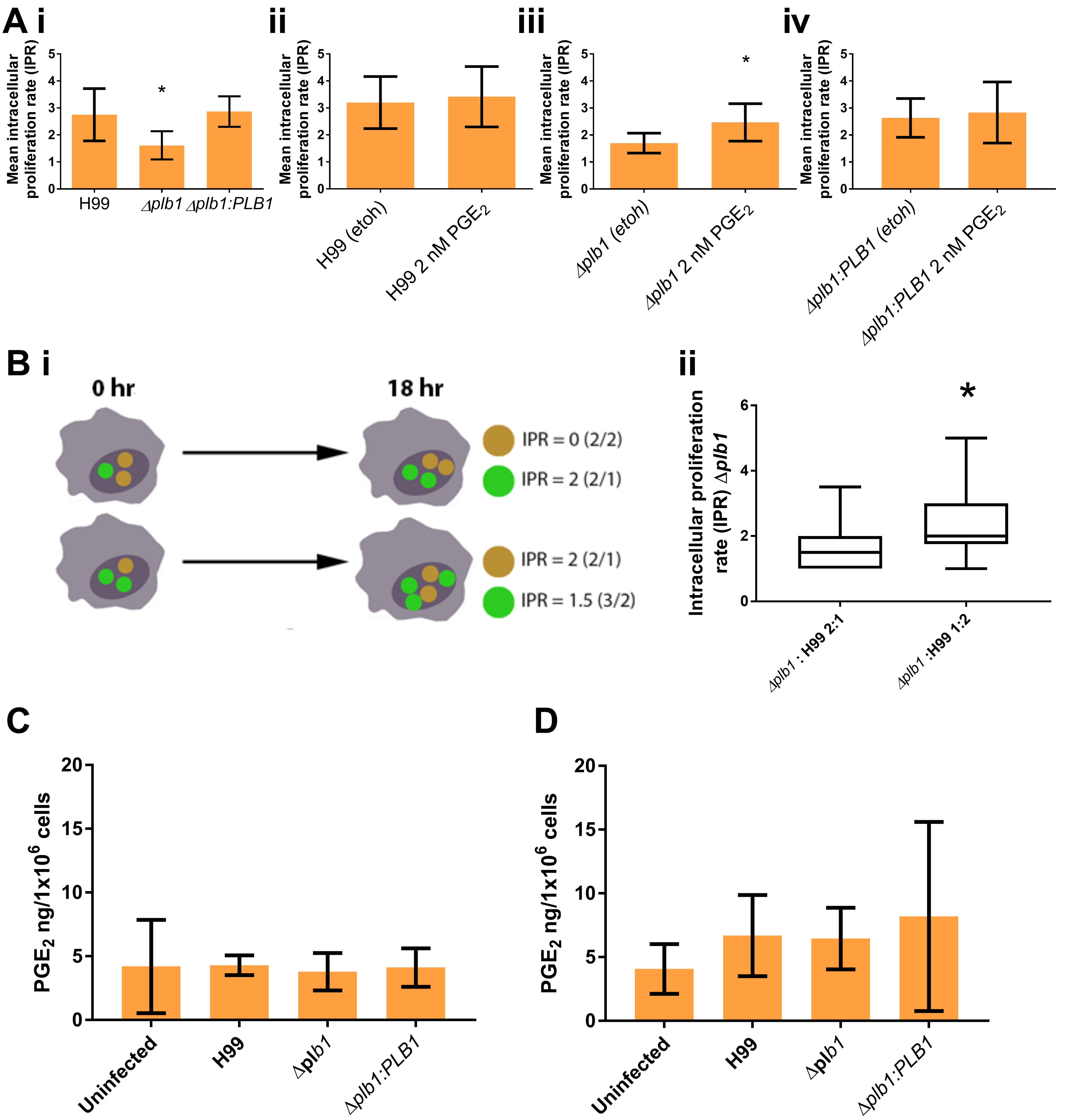
A i
Mean intracellular proliferation rate (IPR)
0
1
2
3
4
5
*
H99
Δplb1
Δplb1:PLB1
ii
Mean intracellular proliferation rate (IPR)
H99 (etoh)
H99 2 nM PGE2
iii
Mean intracellular proliferation rate (IPR)
*
Δplb1 (etoh)
Δplb1 2 nM PGE2
iv
Mean intracellular proliferation rate (IPR)
Δplb1:PLB1 (etoh)
Δplb1:PLB1 2 nM PGE2
B i
0 hr
18 hr
IPR = 0 (2/2)
IPR = 2 (2/1)
IPR = 2 (2/1)
IPR = 1.5 (3/2)
ii
Intracellular proliferation rate (IPR) Δplb1
0
2
4
6
*
Δplb1 : H99 2:1
Δplb1 :H99 1:2
C
PGE2 ng/1x10^6 cells
0
5
10
15
20
Uninfected
H99
Δplb1
Δplb1:PLB1
D
PGE2 ng/1x10^6 cells
0
5
10
15
20
Uninfected
H99
Δplb1
Δplb1:PLB1

H99-GFP

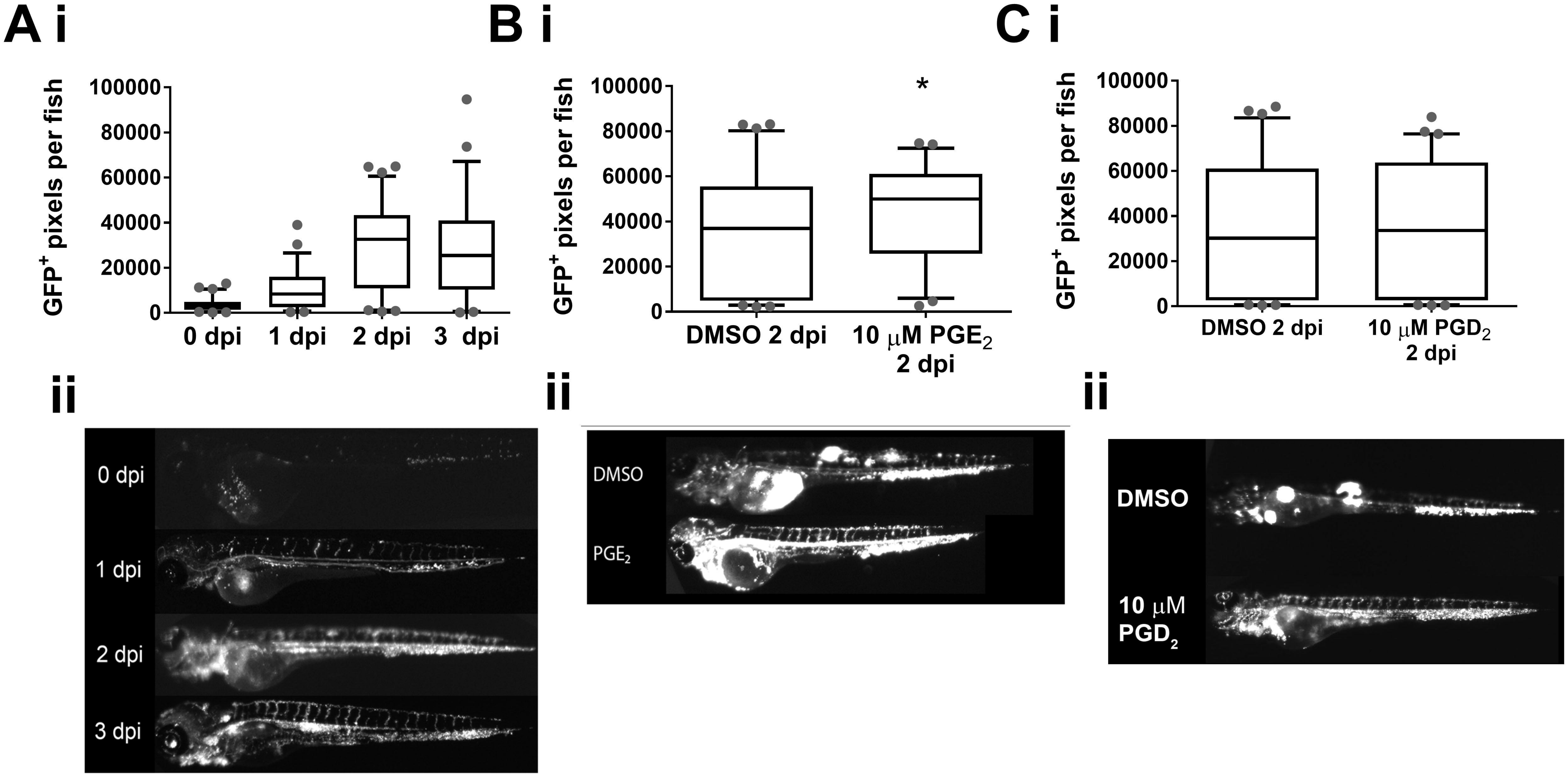

Δplb1-GFP

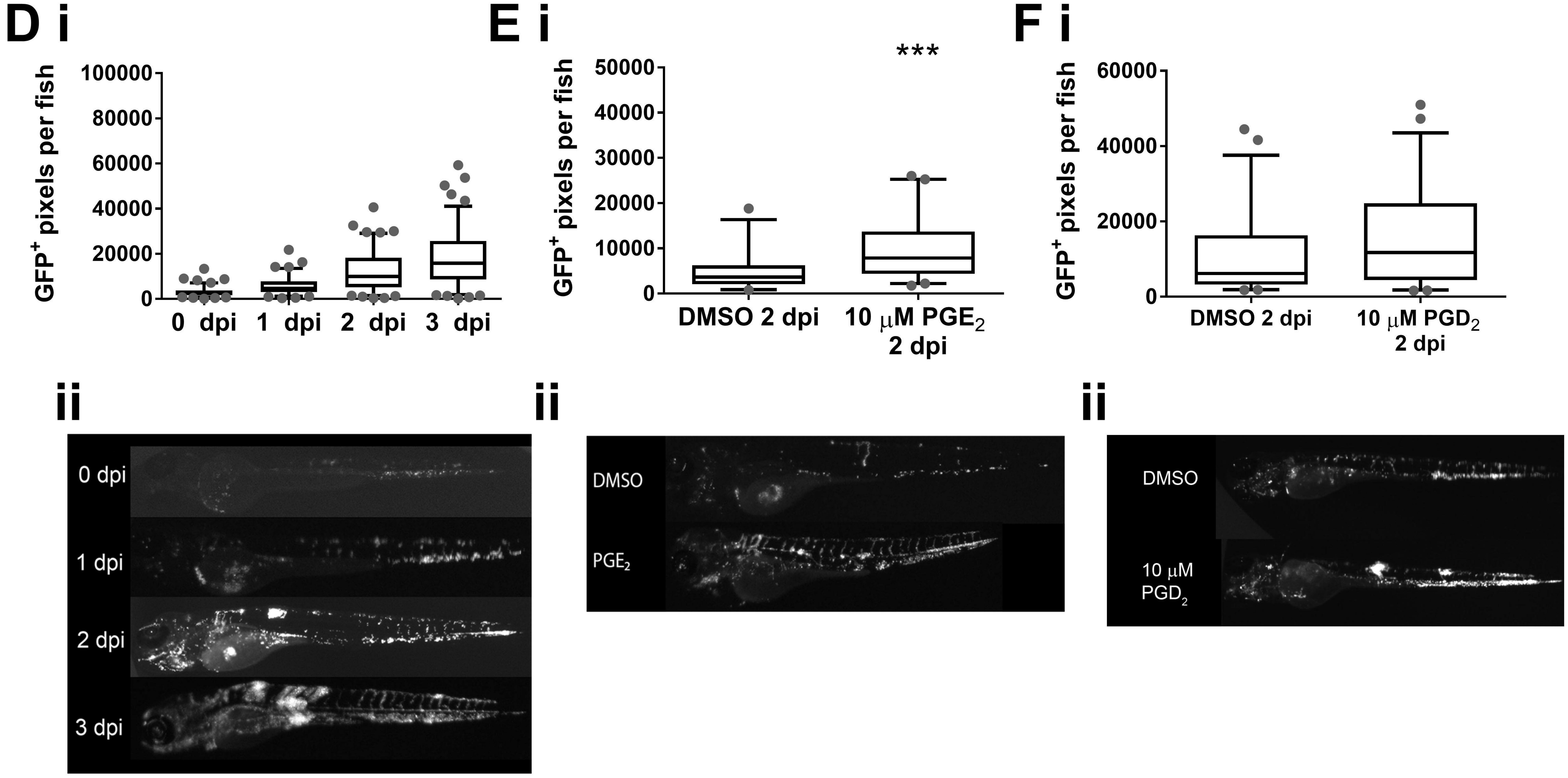

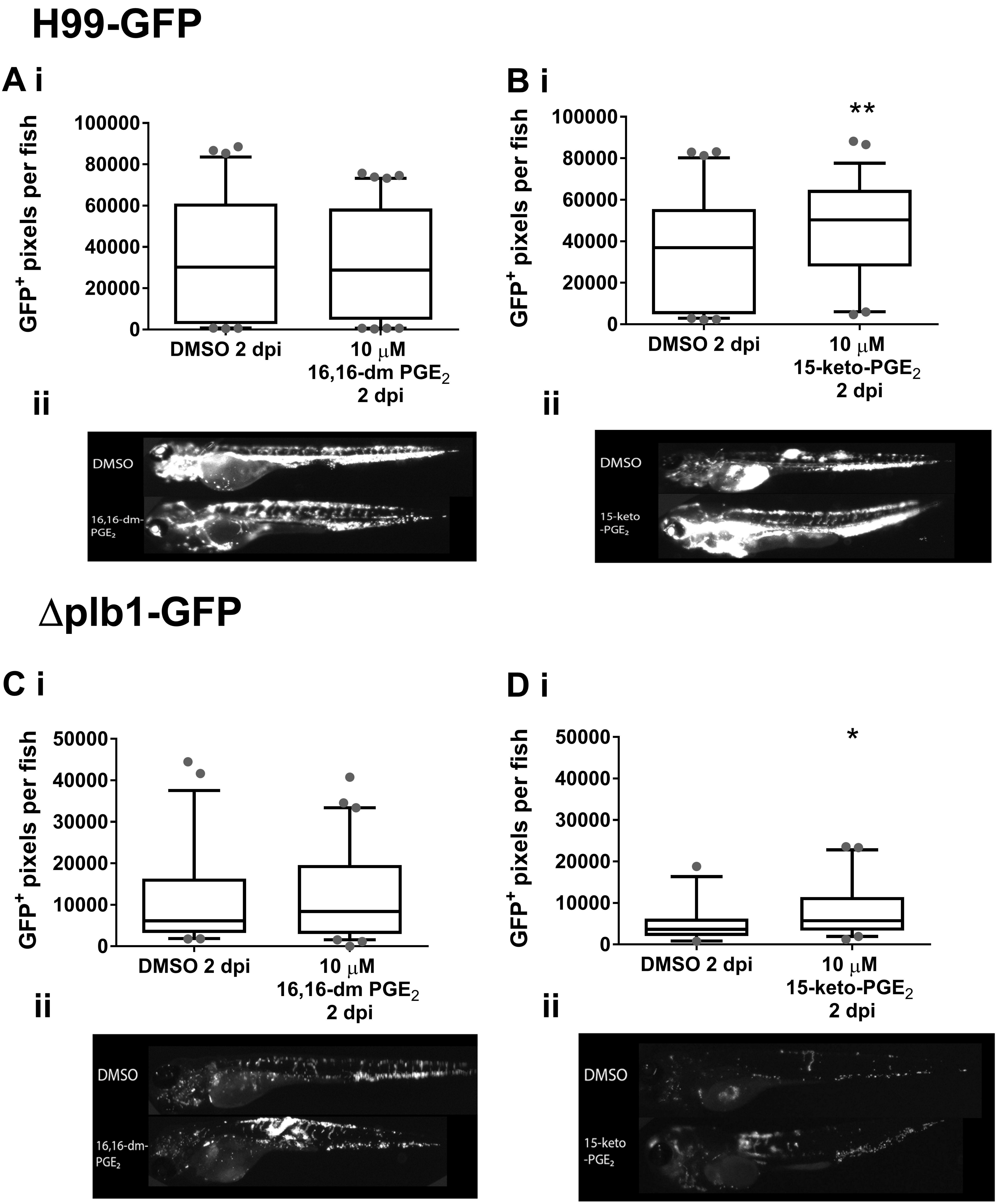
H99-GFP
A i
GFP$^+$ pixels per fish
100000
80000
60000
40000
20000
0
DMSO 2 dpi
10 μM 16,16-dm PGE$_2$ 2 dpi
ii
DMSO
16,16-dm-PGE$_2$
B i
**
GFP$^+$ pixels per fish
100000
80000
60000
40000
20000
0
DMSO 2 dpi
10 μM 15-keto-PGE$_2$ 2 dpi
ii
DMSO
15-keto -PGE$_2$
Δplb1-GFP
C i
GFP$^+$ pixels per fish
50000
40000
30000
20000
10000
0
DMSO 2 dpi
10 μM 16,16-dm PGE$_2$ 2 dpi
ii
DMSO
16,16-dm-PGE$_2$
D i
*
GFP$^+$ pixels per fish
50000
40000
30000
20000
10000
0
DMSO 2 dpi
10 μM 15-keto-PGE$_2$ 2 dpi
ii
DMSO
15-keto -PGE$_2$

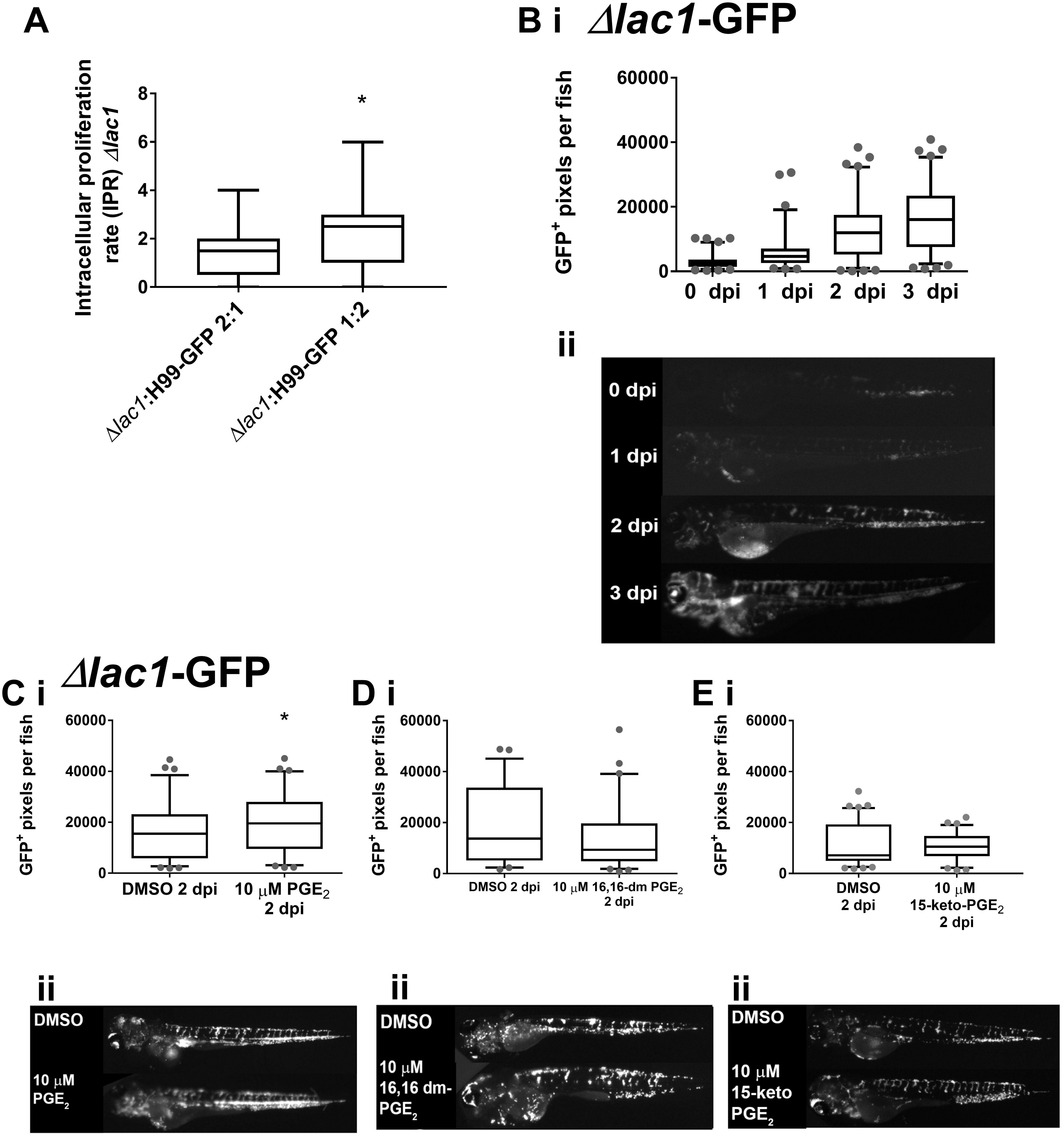
A
Intracellular proliferation rate (IPR) Δlac1
0
2
4
6
8
*
Δlac1:H99-GFP 2:1
Δlac1:H99-GFP 1:2
B i Δlac1-GFP
GFP+ pixels per fish
0
20000
40000
60000
0 dpi
1 dpi
2 dpi
3 dpi
ii
0 dpi
1 dpi
2 dpi
3 dpi
C i Δlac1-GFP
GFP+ pixels per fish
0
20000
40000
60000
*
DMSO 2 dpi
10 μM PGE2 2 dpi
D i
GFP+ pixels per fish
0
20000
40000
60000
DMSO 2 dpi
10 μM 16,16-dm PGE2 2 dpi
E i
GFP+ pixels per fish
0
20000
40000
60000
DMSO 2 dpi
10 μM 15-keto-PGE2 2 dpi
ii
DMSO
10 μM PGE2
ii
DMSO
10 μM 16,16 dm-PGE2
ii
DMSO
10 μM 15-keto PGE2

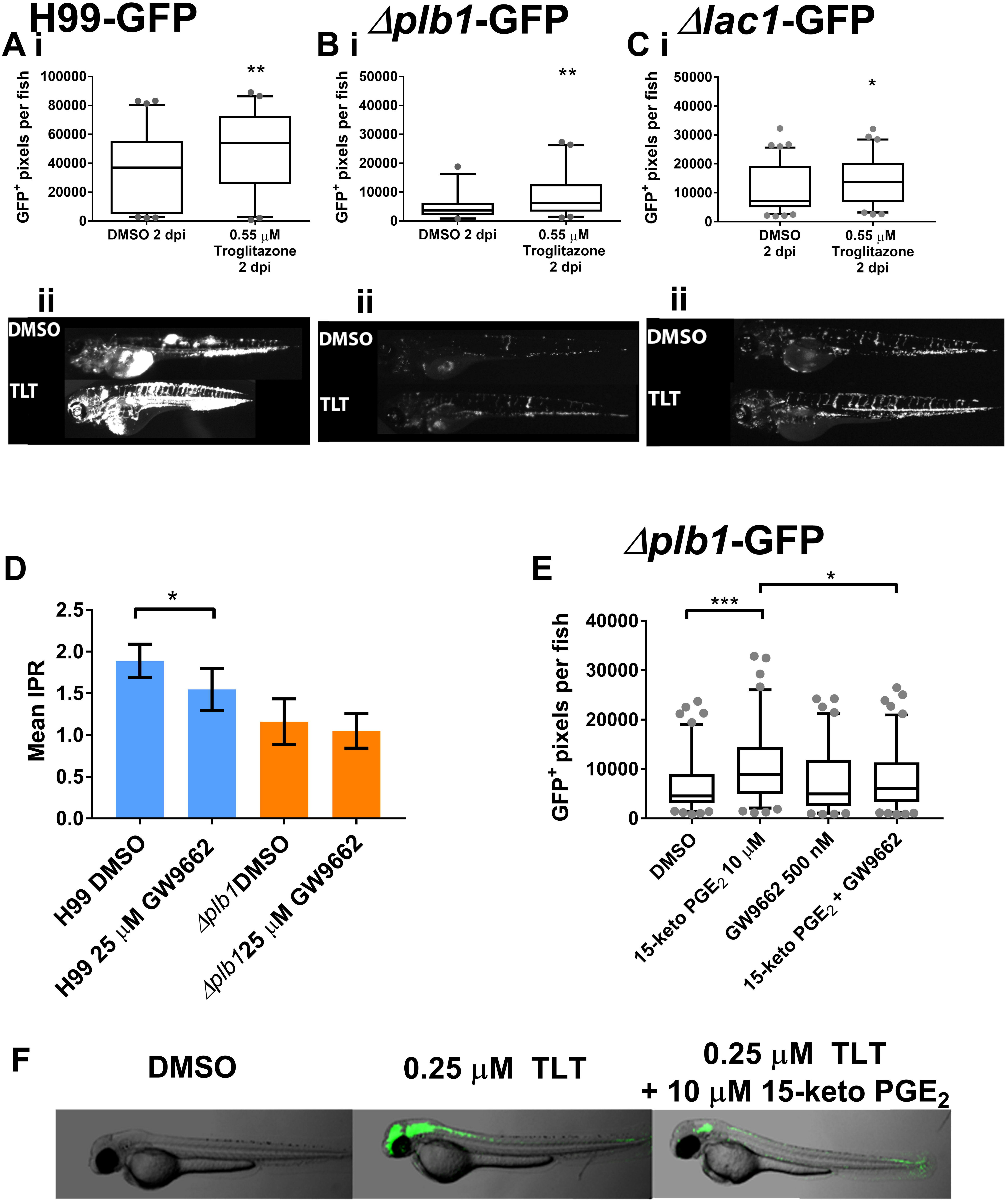
H99-GFP
A i
GFP$^+$ pixels per fish
100000
80000
60000
40000
20000
0
**
DMSO 2 dpi
0.55 μM Troglitazone 2 dpi
Δplb1-GFP
B i
GFP$^+$ pixels per fish
50000
40000
30000
20000
10000
0
**
DMSO 2 dpi
0.55 μM Troglitazone 2 dpi
Δlac1-GFP
C i
GFP$^+$ pixels per fish
50000
40000
30000
20000
10000
0
*
DMSO 2 dpi
0.55 μM Troglitazone 2 dpi
ii
DMSO
TLT
ii
DMSO
TLT
ii
DMSO
TLT
D
Mean IPR
2.5
2.0
1.5
1.0
0.5
0.0
*
H99 DMSO
H99 25 μM GW9662
Δplb1DMSO
Δplb125 μM GW9662
Δplb1-GFP
E
GFP$^+$ pixels per fish
40000
30000
20000
10000
0
***
*
DMSO
15-keto PGE$_2$ 10 μM
GW9662 500 nM
15-keto PGE$_2$ + GW9662
F
DMSO
0.25 μM TLT
0.25 μM TLT + 10 μM 15-keto PGE$_2$